 CMC, vol.8, no.1, pp.33-42, 2008

Thermal Cycling Degradation of T650 Carbon Fiber/PT-30 Cyanate Ester Composite

Huanchun Chen[1] **and Kunigal Shivakumar**[1]

Abstract: Thermal cycling degradation effect on tensile and flexural properties of Cytec T650 carbon/Lonza Primaset PT-30 cyanate ester composite rods used for gas turbine engine brush seals was evaluated. The composite rods were thermal cycled in air from room temperature to 315˚C for 100, 200, 400, 600 and 800 cycles. Each thermal cycle is a one hour period with 28 minutes hold at peak temperature and a high heating/cooling rate of 73˚C/min. The composite withstood the first 100 thermal cycles with less than 10% property change. After that, tensile strength and fracture strain as well as flexural modulus were gradually reduced. Residual properties of the composite rods are expressed in simple equations as a function of the number of thermal cycles. Thermal cycling increased the T_g of the composite rods from 408 ˚C to 468 ˚C. Microcracks, fiber/matrix debonding and matrix loss were observed in the thermal cycled composite rods and are the main reasons for the property degradation. Weight loss study demonstrated loss of material due to matrix degradation.

Keyword: Pultruded composites, PT-30 cyanate ester, thermal cycling, mechanical properties, environmental degradation

1 Introduction

Recently, a new brush seal concept was proposed [Holloway et al. (2006)] to improve the engine performance. This brush seal was made up of Cytec T650 carbon fiber/Lonza Primaset PT-30 cyanate ester pultruded composite rods of 0.5 mm diameter. PT-30 cyanate ester resin was selected because of its low moisture absorption, good fracture toughness, favorable dielectric properties and excellent processing characteristics [Abali et al. (2003), Hemerton (1994)]. The effects of engine environment involving lubricant fluids soaking and cyclic thermal loading on the integrity of the carbon fiber/PT-30 composite rods are major concerns and decide the durability and the life of the seal. Engine lubricating fluids effect on this composite rod has been studied by Shivakumar et al. [Shivakumar et al. (2008)]. The effect of thermal cycling is the main focus of this paper.

Thermal cycling effects on uni- and multi-directional polymer composite laminates have been studied extensively. The results showed that microcracking [Hancox (1998), Shimokawa et al. (2002), Lee (2001)] and fiber/matrix debonding [Lafarie-Frenot et al. (2004)] are the most common failure modes observed in composite laminates subjected to thermal cycling. Thermal cycling resulted in weight loss [Lee et al. (2001), Chung et al. (2000), Lafarie-Frenot (2006)] and degradation of tensile, compressive, shear and flexural strength and modulus [Sinmazcelik et al. (2006), Cao et al. (2005), Lee et al. (1996)]. The deterioration in mechanical properties was attributed to a combination of thermal stresses induced by the difference in coefficient of thermal expansion (CTE) and thermal oxidation/degradation when the composite is exposed to an oxidative atmosphere [Chernin et al. (2004)]. A few researchers [Dutta (1988), Kern (1990)] reported increased tensile strength and modulus, which they attributed to stress relief due to internal cracking. All the composites considered in the above studies were laminates. No research has been reported on thermal cycling of pultruded rods and/or Primaset PT-30 cyanate ester composites.

[1] Center for Composite Materials Research, Department of Mechanical and Chemical Engineering, North Carolina, A&T State University. E-mail: kunigal@ncat.edu

The objective of this paper is to evaluate the thermal cycling degradation effect on tensile and flexural properties of T650 carbon/Lonza Primaset PT-30 cyanate ester composite rods manufactured by pultrusion process. The composite rod is 0.5mm $\pm$ 0.01mm in diameter and is chosen for use in new brush seals [Holloway et al. (2006)]. Currently there is no ASTM standard simulating the engine environment conditioning. Therefore a common working knowledge in that industry is used. The rods are exposed to thermal cycling from room temperature (RT) to 315˚C in air at the frequency of 1 hour/cycle for 100, 200, 400, 600 and 800 cycles. Tension and three-point bend flexure tests are conducted. Residual tensile and flexural properties for different number of thermal cycles are obtained and compared. Cross-sectional morphology is examined to evaluate the microstructural change of the rods. Glass transition temperature (T_g) change due to thermal cycling is measured by Dynamic Mechanical Analysis (DMA). Weight loss study is performed to compare the effect of thermal cycling with that of isothermal condition.

2 Materials

The materials considered are Cytec T650 carbon fiber (3k tow) and Primaset PT-30 cyanate ester supplied by Lonza Corporation. PT-30 is a thermoset resin that has 65% char yield (same as phenolics) and less than 0.5% volatiles and generates no gaseous by-products during cure. PT-30 has a low viscosity (80c.p.s.) at its processing temperature (120˚C) and is post-curable to achieve T_g in excess of 371˚C. It has excellent electrical and dielectrical properties and thermo-mechanical stabilities.

3 Manufacturing of Composite Rods

The composite rods were manufactured by pultrusion process. Pultrusion is a highly automated process for manufacturing composite material parts of constant cross-section shaped profiles. The process consists of guiding the T650 fiber tow from a creel through a set of guides, and then pulling through a PT-30 resin bath that is maintained at a proper temperature so that the tow is adequately impregnated with the resin. The impregnated fiber tow is then pulled through a hot die, where the tow is shaped into a circular shape. Finally the rod is pulled through a thermal curing chamber to complete the curing first at 260˚C for two minutes and then at 315˚C for another two minutes. The fully cured fiber rod is collected by the take up spool. Using the above process, Aztex Inc. produced the rods and supplied in lengths of 300 mm. Optical microscopic image showed that the fiber volume fraction of the rod is about 65% $\pm$ 1%. This high fiber volume fraction is expected in a pultrusion process.

4 Thermal Cycling

Each thermal cycle is a one-hour period containing hold at room temperature (RT) for 12 minutes, heat-up from RT to 315˚C in 4 minutes, hold at 315˚C for 28 minutes, cool-down from 315˚C to RT in 4 minutes and finally hold at RT for another 12 minutes. A special heating and cooling apparatus was designed and built to achieve the rapid heating and cooling rates (73˚C/min). Figure 2 shows the proposed (dashed line) and actual (solid line) temperature profiles for each cycle. The actual cycle achieved almost duplicated the proposed cycle. The only difference is that the actual heating and cooling ramps were 4 minutes instead of 2 minutes.

Six sets of five numbers each of 300mm pultruded rods were chosen. One set was set aside for baseline properties test. The remaining five sets were thermal cycled for 100, 200, 400, 600 and 800 cycles and then tested for mechanical properties.

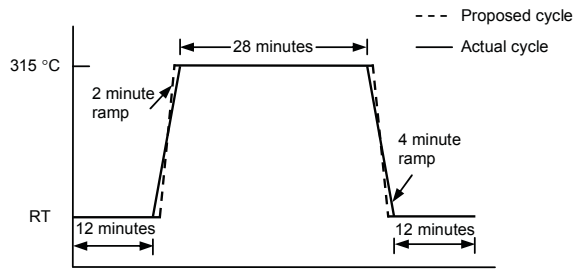

Figure 2: Proposed and actual thermal cycles

5 Microscopy of Pultruded Composite Rods

Optical microscope and Scanning Electron Microscope (SEM) analyses were conducted on baseline (as received) samples as well as samples that were thermal cycled for 100, 200, 400, 600 and 800 cycles to investigate the thermal cycling effect on the morphology of the composite rods.

5.1 As-received (baseline) Composite Rods

Figure 3 shows the optical microscopic images of the baseline rod cross-section. Figure 3(a) displays the whole rod cross-section and 3(b) shows the details of fiber distribution. Fibers are uniformly and densely distributed and are well bonded to the resin except at some dark regions indicating voids or resin deficiency. The microscopy examination was repeated at five cross-sections of each rod and for five rods. All the images showed the same trend.

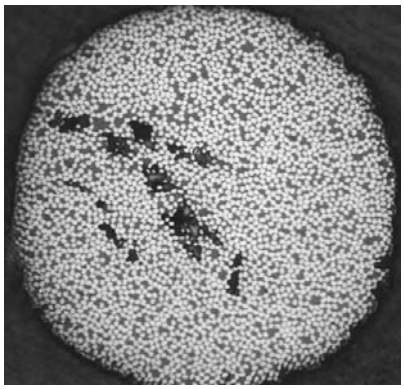

(a) Whole rod cross-section (x200)

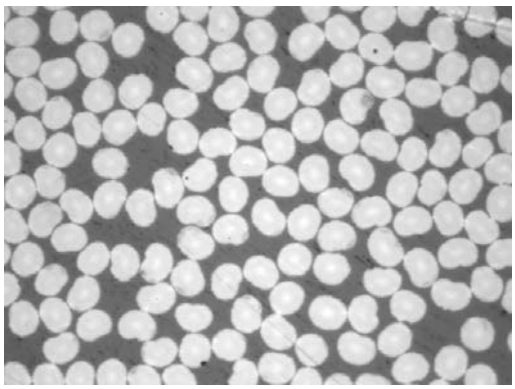

(b) Details of fiber distribution (x1k)

Figure 3: Optical microscopic images of baseline rod cross-section

5.2 Thermal Cycled Composite Rods

Figure 4 shows the progressive morphology change as the number of thermal cycles increases from 100 to 800. The rod cycled for 100 cycles looks almost the same as the as-received rod (See Figure 4(a)). After 200 thermal cycles (see Figure 4(b)), microcracks and small cavities in the matrix can be observed. When increasing the number of thermal cycles to 400 cycles, widespread fiber/matrix debonding and matrix shrinkage are found (see Figure 4(c)). Finally, after 800 thermal cycles (see Figure 4(d)), fiber/matrix separation and signs of matrix loss appear around almost every fiber in the rod.

The morphology change of the composite rods is the result of combined effects of thermal stress and possible matrix degradation/oxidation. Under the thermal cycling condition, the coefficient of thermal expansion (CTE) mismatch between fiber and matrix results in thermal stress at the fiber/matrix interface. This repeated thermal stress cycle could initiate fiber/matrix debonding. As thermal cycling continues, the increase in the interface area creates a path that helps the diffusion of the oxygen into the composite and thus accelerates the matrix degradation. The fiber/matrix debonding and microcracks propagation can be simulated by different numerical models [Wang et al. (2006), Han et al. (2006)].

6 Glass Transition Temperature (T_g)

Glass Transition Temperature (T_g) of Dynamic mechanical analysis (DMA) was performed using DMA 7e from Perkin Elmer to measure the glass transition temperature (T_g) of the baseline and 600 thermal cycled composite rods. The specimen was tested under 3-point bending. The specimen span was 20 mm and the central load applied was about 150 mN. Temperature scan test was conducted at 5˚C/min with the frequency of 1 Hz. Storage modulus, loss modulus and damping factor (Tanδ) were measured continuously with temperature. Using the storage modulus data, T_g was calculated as per ASTM standard E 1640-04. The T_g of four baseline samples ranged from 396˚C to 416˚C (same as PT-30 data) with an av-

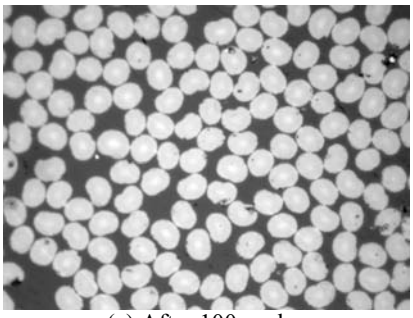

(a) After 100 cycles

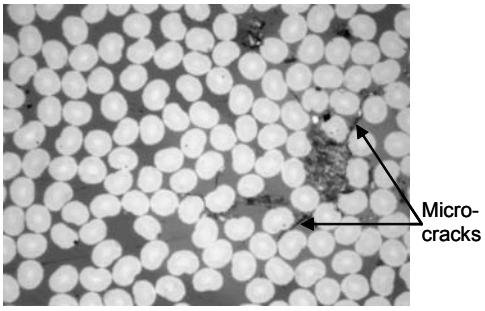

(b) After 200 cycles

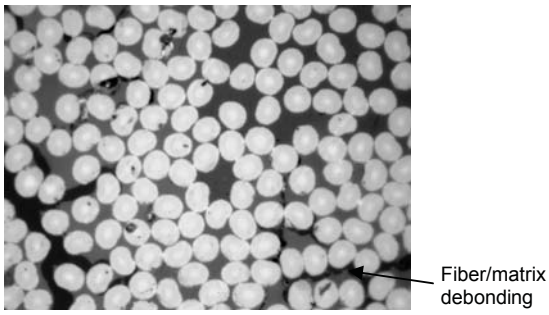

(c) After 400 cycles

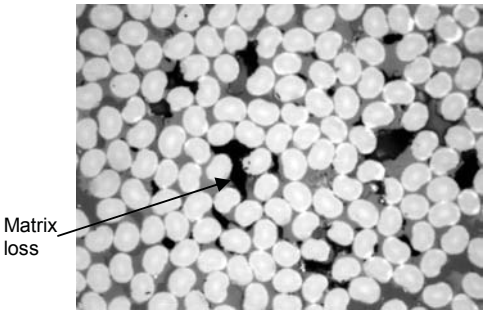

(d) After 800 cycles

Figure 4: Optical microscopic images of rod cross sections after thermal cycling

erage of 408˚C. 600 thermal cycles increased the T_g by 60˚C to 468˚C, demonstrating the fact that the heat treatment does increase the T_g, as evidenced in many thermoset polymer composites.

7 Tensile and Flexural Properties of Pultruded Composite Rods

Tension and flexure tests were conducted on baseline and thermal cycled specimens to measure the mechanical properties degradation of the composite rods. Tensile modulus, strength and fracture strain were measured by a specially designed tension fixture. Flexural stiffness/ modulus loss was measured by a three-point bend flexure test.

7.1 Tension Test

The tension test specimen configuration is shown in Figure 5. The total length of the specimen was 300 mm and the tab length was 25.4 mm. The composite rod diameter was 0.5 mm with $\pm$ 0.01 mm in variation. The test-length L, which was approximately 254 mm, was measured to the nearest 0.025 mm for each specimen. Because of the small size of the rod, a special tabbing system was devised. The ends of the composite rod specimen were inserted and bonded to 3.175 mm OD aluminum tubes using Scotch-Weld Epoxy Adhesive DP-460.

The specimen was gripped by double-angle collet grips over the aluminum tube tabs. Figure 6 shows the schematic of the test setup. The details of the tabbing and test setup were described by Shivakumar et al. [Shivakumar et al. 2008].

A load cell with a full-scale range of 1 kN was chosen for the tests. Load was recorded to the nearest 0.04 N. An LVDT was used to directly measure the change in displacement between the two grips, thus eliminating the load-train deformation if the actuator displacement had been used. The tests were run at a constant displacement rate of 0.5 mm/min. The load and displacement were recorded continuously (every $1/2$ second) during the test. The strain was calculated by dividing the displacement by the initial test-length of the specimen. Tensile stress was calculated by dividing the load by the cross-sectional area of the circular rod. The test was continued until the specimen fractured. For each test specimen, the complete stress-strain response from

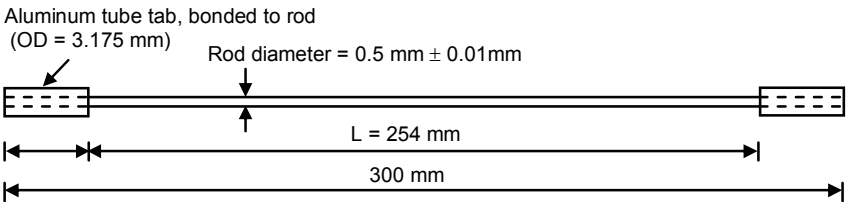

Figure 5: Tension specimen configuration

zero load until failure was acquired. This data gave us strength, modulus, and fracture strain of the test specimen. The stress-strain response for all specimens was found to be linear until the fracture. Five specimens were tested for each case.

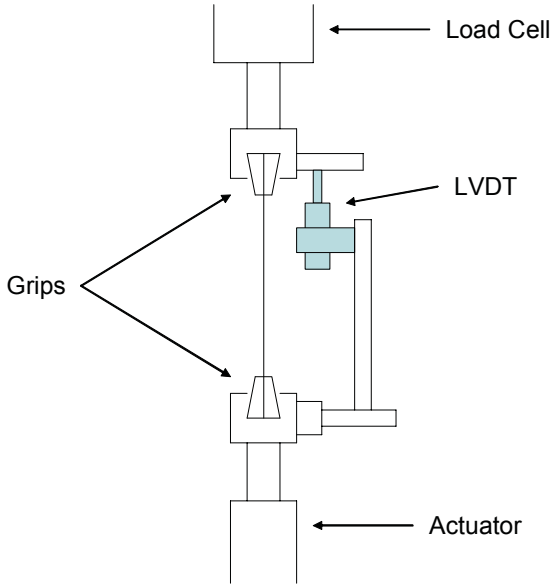

Figure 6: Schematic of tension test setup

The tension test results for baseline and thermal cycled rods are summarized in Table 1. The average (average of five tests) values of tensile strength, modulus and fracture strain for each case, percent CV (coefficient of variation) and percent change from baseline are listed. The percent CV is reasonable for all conditions. The tensile strength of baseline composite rods is 1.76 GPa, modulus is 138 GPa and fracture strain is 1.27%. Tensile strength and strain were gradually degraded by thermal cycling. The loss of tensile strength is 7, 16, 22, 27 and 36%, respectively for 100, 200, 400, 600 and 800 thermal cycles. The loss of fracture strain is of the same order as that of strength. The modulus of the composite rods was almost unaffected. Based on these results one can conclude that T650/PT-30 composite rods can withstand 100 thermal cycles with practically no loss of stiffness and strength. However, after 800 thermal cycles, the composite lost 36% tensile strength and 28% ultimate strain.

Figure 7 displays the residual tensile strength versus the number of thermal cycles. Error bars on each data point represent the minimum and maximum values, while the data point represents the average value for the case, normalized to the baseline value. The residual tensile strength decreased linearly with square root of the number of thermal cycles. Their relationship after 100 thermal cycles can be expressed by Eq (1):

$$\frac{S}{S_0} = 1.07 - 0.015N^{1/2} \tag{1}$$

Where S and N represent the residual tensile strength and the number of thermal cycles, respectively. The subscript '0' represents the baseline property. Post-test photos in Figure 8 illustrate typical tensile failures for baseline and thermal cycled test samples. Baseline test samples showed brittle fracture typical of unidirectional carbon composites. All thermal cycled test samples showed splintering (shattering) of fibers due to degraded matrix properties.

7.2 Flexure Test

The purpose of this test is to evaluate the extent of matrix damage due to thermal cycling exposure of the composite rods. The matrix damage due to micro-cracking and interfacial separation should affect the flexural modulus/stiffness much more readily than the tensile modulus. Therefore

Table 1: Tensile properties vs. number of thermal cycles

Number of Cycles	Tensile Strength		Tensile Modulus		Fracture Strain	
	Strength (GPa)	% change	Modulus (GPa)	% change	Strain (%)	% change
0	1.76 (4.1*)	0	138 (0.9*)	0	1.27 (3.8*)	0
100	1.62 (2.5)	-7%	129 (0.8)	-6%	1.26 (2.9)	-1%
200	1.48 (3.3)	-16%	124 (2.7)	-10%	1.17 (1.7)	-8%
400	1.37 (4.2)	-22%	126 (3.1)	-8%	1.09 (6.3)	-14%
600	1.29(6.5)	-27%	144 (0.8)	+5%	0.91 (6.7)	-28%
800	1.12 (6.0)	-36%	125 (2.5)	-9%	0.91 (4.9)	-28%

* Percent Coefficient of Variation

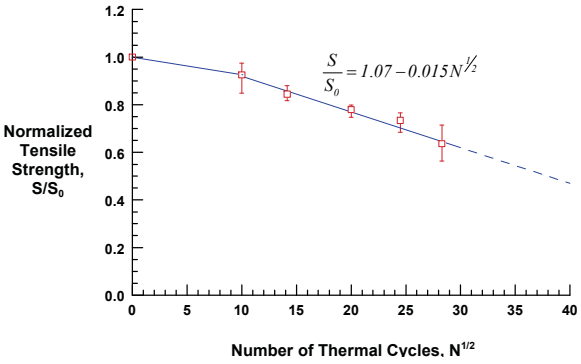

Figure 7: Degradation of tensile strength with thermal cycling

(a) Baseline sample

(b) Thermal cycled sample

Figure 8: Typical tensile failure modes

a three-point bend test (As per ASTM D2344), with a span to diameter ratio of 30, was chosen. The test setup and the specimen are shown in Figure 9.

For each sample category, three of the 300 mm rods were used for the flexure tests. From each of these three rods, the flexure specimens were cut as three 25.4 mm segments from one end of the rod and tested. A total of nine specimens were tested

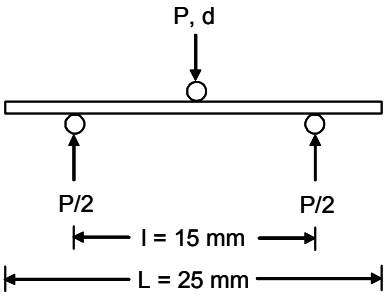

Figure 9: Schematic of flexure test setup

for each thermal cycling case.

A small precision bending fixture was used for the test. The lower loading supports were 3.175 mm diameter and the upper support was 6.35 mm diameter. Load data was acquired with a resolution of 0.004 N $\pm$ 0.002 N. The displacement loading rate was 0.5 mm/min.

Figure 10 shows typical flexure load-displacement plots for baseline and thermal cycled specimens. For baseline specimens, the load drops each time a group of fibers fails (See Figures 10(a) and 10(b)). For the thermal cycled specimens, fibers in the rod reoriented themselves from circular to an elliptical shape during failure (See Figure 10(c)). The reorientation of fibers is caused by the fiber-matrix interfacial separation and matrix damage as shown previously through microscopic images in Figure 4.

The flexure test determined both the maximum load and the stiffness of the test specimen. The stiffness change from non thermal cycled to thermal cycled measured the effect of thermal cycling. The stiffness is defined as the slope of the load vs. displacement plot, $K_b = \Delta P/\Delta d$, as illustrated in

Figure 10(a).

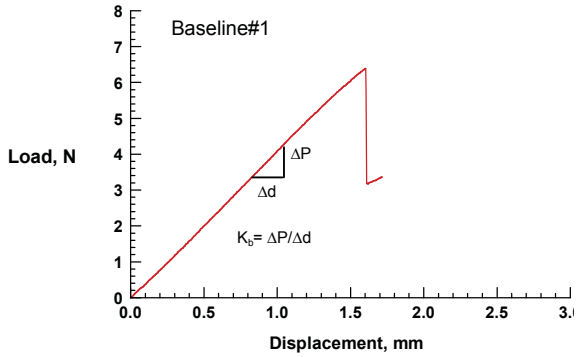

(a) Baseline sample #1

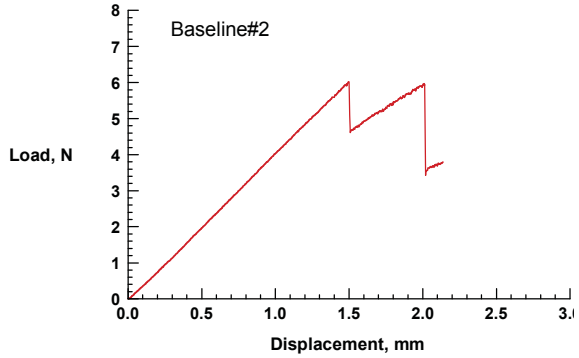

(b) Baseline sample #2

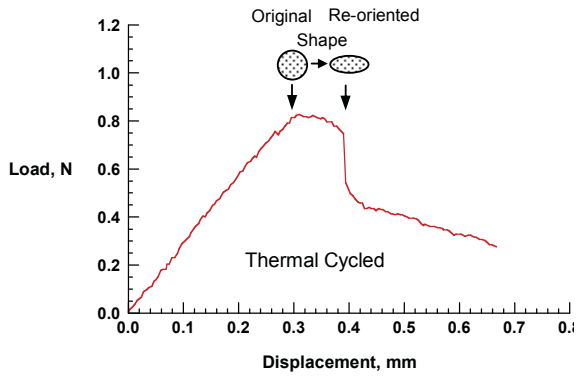

(c) Thermal cycled sample

Figure 10: Load-displacement responses of typical flexure test

Flexural modulus $E_b$can be calculated from the stiffness K_b using equation (2):

$$E_b = \frac{4l^3 K_b}{3\pi D^4} \tag{2}$$

Where l is the span of three-point bend test, D is the rod diameter and K_b is the flexural stiffness as defined in Figure 10(a). Table 2 summarizes the flexure test results for baseline and 100, 200, 400, 600 and 800 thermal cycles conditions. The average values of maximum or fracture load, flexural modulus and stiffness for each case, percent coefficient of variation (within the parenthesis) and the property change from baseline are listed. Thermal cycling significantly reduced the failure load after 200 cycles. The maximum load was reduced by 31% for 200 thermal cycles and by 86% for 800 thermal cycles. For 100 and even 200 thermal cycles, there was no loss of flexural modulus. After 200 cycles, the modulus/stiffness loss steadily increased. The flexural modulus/stiffness decreased by 28% after 800 cycles. The large reduction in failure load and modulus indicates a possible material degradation/oxidation due to thermal cycling. The normalized flexural modulus (E_b/E_0) versus the number of thermal cycles is shown in Figure 11, where E_b is the flexural modulus of the thermal cycled specimen and E_0 is that of the baseline specimen. The modulus loss (E_b/E_0) can be approximated using Equation (3):

$$\frac{E_b}{E_0} = 0.7 + \frac{0.3}{1 + 2 \times 10^{-15} N^{5.6}} \tag{3}$$

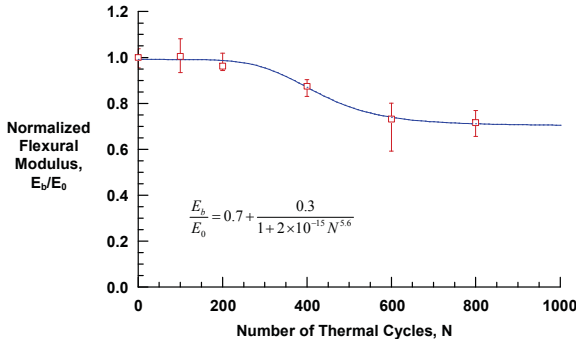

Figure 11: Degradation of flexural modulus with thermal cycling

Table 2: Flexural properties vs. number of thermal cycles

Number of Cycles	Maximum Load		Flexural Properties		
	Load (N)	% change	Modulus (GPa)	Stiffness (N/mm)	% change
0	6.51 (9.7*)	0	125 (2.6*)	4.06 (2.6*)	0
100	6.32 (2.7)	-3%	126 (4.0)	4.08 (4.0)	0%
200	4.48 (12.7)	-31%	120 (2.5)	3.91 (2.5)	-4%
400	2.27 (15.3)	-65%	109 (2.7)	3.55 (2.7)	-13%
600	1.15 (25.4)	-82%	91.5 (9.1)	2.97 (9.1)	-27%
800	0.89 (9.3)	-86%	89.7 (5.3)	2.91 (5.3)	-28%

* Percent Coefficient of Variation

8 Weight Loss of PT-30 Resin and T650/PT-30 Composite Rod Under Isothermal and Thermal Cycling Conditions

In order to evaluate the thermal degradation of the T650/PT-30 pultruded composite rods due to thermal cycling versus isothermal exposure, a weight loss study was performed on PT-30 resin and T650/PT-30 composite rods isothermally at 315˚C in the presence of air for 300 hours. This isothermal condition simulates the cumulative hold time at the elevated temperature during the 600 thermal cycles. The PT-30 resin sample was prepared by curing at 200˚C for 6 hours and then postcuring at 260˚C for 8 hours. PT-30 resin and composite rod samples were placed in an oven maintained at 315˚C. The weights of the samples were measured at every 24 hours interval. Figure 12 illustrates the percent residual weight (W/W_0) versus the exposure time in hours for PT-30 resin and T650/PT-30 composite rods.

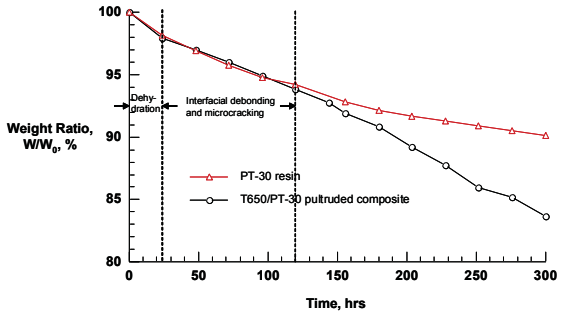

Figure 12: Weight ratio versus time of PT-30 resin and T650/PT-30 pultruded composite

Both PT-30 resin and T650/PT-30 composite samples displayed steady weight loss. The weight loss is the sign of additional postcuring and thermal degradation/oxidation of the resin. Both reactions can generate volatiles and cause the weight loss. In the first 24 hours period, the resin and the composite showed a high weight loss rate, which is the result of rapid dehydration. After that, both samples experienced steady weight loss at a lower rate than the first 24 hours. During this period, thermal degradation mainly occurred at the surfaces of the samples. Microcracks and fiber/matrix debonding started to form in the composite sample. The resin and the composite degraded at almost the same rate. After 120 hours, the composite weight loss rate increased while the PT-30 rate decreased. PT-30 resin showed 10% weight loss after 300 hours, while the composite lost 16% of the weight. The reason for the accelerating weight loss rate of the composite might be the microcracks and fiber/matrix debonding which created more reactive surface areas and paths for oxygen to diffuse thus increased the resin degradation rate. Parvatareddy et al. [Parvatareddy et al. (1995)] also noticed that the composite samples lost much more weight than unreinforced resin specimens over the same aging period.

Furthermore, the T650/PT-30 composite rods thermal cycled for 600 cycles showed almost the same weight loss (17%) as that under the 300 hours isothermal condition (16%). This shows that the thermal cycling degradation effect can be represented by the cumulative sum of isothermal oxidation effect at the peak temperature, which was also noted by Lee and Holl [Lee et al. (1996)] for $(+45/-45)_s$ laminate.

9 Concluding Remarks

This paper evaluated the thermal cycling degradation effect on tensile and flexural properties of Cytec T650 carbon/Lonza Primaset PT-30 cyanate ester pultruded composite rods used for gas turbine engine brush seals. Each thermal cycle is a one hour period including 24 minutes of hold at room temperature, 28 minutes of hold at 315˚C and 4 minutes each of heating and cooling ramps. The heating/cooling rate is 73˚C.

Tension and flexure tests were conducted on non thermal cycled and thermal cycled samples for 100, 200, 400, 600 and 800 cycles. Tensile strength, strain and modulus as well as flexural modulus and failure load were measured and compared with each other. The composite rods survived the first 100 cycles with less than 10% properties changes. After that, thermal cycling gradually reduced tensile strength and fracture strain of the composite rods while tensile modulus remained almost unchanged. Residual tensile strength can be expressed as a function of the number of thermal cycles by equation $\frac{S}{S_0} = 1.07 - 0.015N^{1/2}$. Flexural failure load and modulus were severely reduced by thermal cycling. The flexural modulus did not change during the first 100 cycles and then decreased following the equation $\frac{E_b}{E_0} = 0.7 + \frac{0.3}{1+2\times10^{-15}N^{5.6}}$. After 200 thermal cycles, microcrack, fiber/matrix debonding and matrix loss were observed in the composite rods. They are the main reasons for the tensile strength and flexural modulus degradation.

Thermal cycling the composite rods increased T_g and weight loss. The T_g increased from 408 ˚C to 468 ˚C. The weight loss was about 17% in 600 cycles, which is equivalent to 300 hours of isothermal heating at 315 ˚C. The effect of the two was found to be the same. This confirmed the previous results that the effect of thermal degradation in thermal cycling can be represented by cumulative sum of isothermal degradation at the peak temperature.

Acknowledgement: The authors thank the US Air Force and Gary Holloway of Diversitech Inc. for funding this work through the contract # 10-JE0507. The authors acknowledge Matthew Sharpe and John Skujins of CCMR for their support and Dr. Zhigang Xu of CAMSS for the help with SEM.

References

Abali F., Shivakumar K.N., Hamidi N., Sadler, R. (2003): An RTM densification method of manufacturing carbon-carbon composites using primaset PT-30 resin, *Carbon,* Vol. 41, pp. 893-901.

Cao J., Chen L. (2005): Effect of Thermal Cycling on Carbon Fiber-Reinforced PPS Composites, *Polymer Composites*, Vol. 26, No. 5, pp. 713-716.

Chernin L., Volokh, K.Y. (2004): Simulation of Thin Film Delamination Under Thermal Loading, *CMC: Computers, Materials & Continua*, Vol.1, No.3, pp. 259-273.

Chung K., Seferis J.C., Nam J.D. (2000): Investigation of Thermal Degradation Behavior of Polymeric Composites: Prediction of Thermal Cycling Effect From Isothermal Data, *Composites: Part A*, Vol. 31, pp. 945-957.

Dutta P.K., Kalafut J., Lord H.W. (1988): *ASME* Vol. 9, pp. 192-197.

Han R., Ingber M.S., Schreyer H.L. (2006): Progression of failure in fiber-reinforced materials, *CMC: Computers, Materials & Continua*, Vol.4, No.3, pp.163-176.

Hancox N.L. (1998): Thermal Effects on Polymer Matrix Composites: Part 1, Thermal Cycling, *Materials and Design*, Vol. 19, pp. 85-91.

Hemerton I. (1994): *Chemistry and Technology of Cyanate Ester Resins*, Blackie Academic & Professional, London, UK.

Hillermeier R.W., Seferis J.C. (2000): Environmental Effects on Thermaplastic and Elastomer Toughened Cyanate Ester Composite Systems, *Journal of Applied Polymer Science*, Vol. 77, pp. 556-567.

Holloway G., Mehta J., Rosado L., Doak D., Hubley C., Askew J., Krawiecki, S. (2006): Innovative Rotating Intershaft Brush Seal for Sealing Between Rotating Shafts, Part I-Mechanical Design of the Rotating Brush Seal, AIAA-

2006-4751, 42nd AIAA/ASME/SAE/ASEE Joint Propulsion Conference & Exhibit, 9-12 July 2006, Sacramento, California.

Kern K.T., Long E.R., Long S., Harries W.L. (1990): *Polymer preprints*, AXS, Vol. 31, pp. 611-612.

Lafarie-Frenot M.C., Rouquie S. (2004): Influence of Oxidative Environments on Damage in C/Epoxy Laminates Subjected to Thermal Cycling, *Composites Science and Technology*, Vol. 64, pp. 1725-1735.

Lafarie-Frenot M.S., Rouquie S., Ho N.Q., Bellenger V. (2006): Comparison of Damage Development in C/Epoxy Laminates During Isothermal Ageing or Thermal Cycling, *Composites: Part A*, Vol. 37, pp. 662-671.

Lee B.L., Holl M.W. (1996): Effects of Moisture and Thermal Cycling on In-Plane shear Properties of Graphite Fibre-Reinforced Cyanate Ester resin Composites, *Composites: Part A*, Vol. 27, pp. 1015-1022.

Lee S., Nam J., Ahn K., Chung K. and Seferis J. (2001): Thermo-Oxidative Stability of High Performance Composites under Thermal Cycling Conditions, *Journal of Composite Materials*, Vol. 35 No. 5, pp. 433-454.

Parvatareddy H., Wang J.Z., Dillard D.A., Ward T.C. (1995): Environmental Aging to High-Performance Polymeric Composites: Effects on Durability, *Composites Science and Technology*, Vol. 53, pp. 399-409.

Shimokawa T., Katon H., Hamaguchi Y., Sanbongi S. and Mizuno H. (2002): Effect of Thermal Cycling on Microcracking and Strength Degradation of High-Temperature Polymer Composite Materials for Use in Next-Generation SST Structures, *Journal of Composite Materials*, Vol. 36, No. 7, pp. 885-895.

Shivakumar K., Chen H., Holloway G. (2008): Gas Turbine Environment Effect on Morphology and Mechanical Properties of Pultruded Composite, *Journal of Applied Polymer Science*, Vol. 108, pp. 189–198.

Sinmazcelik T., Arici A.A. (2006): Thermal Cycles Effects on Interlaminar Shear Strength (ILSS) and Impact Behaviour of Carbon/PEI Composites, *Journal of Materials Science*, Vol. 41, pp. 1233-1241.

Wang P.B., Yao Z.H., Lei T. (2006): Analysis of Solids with NumerousMicrocracks Using the FastMultipole DBEM, *CMC: Computers, Materials & Continua*, Vol.3, No.2, pp.65-75.